Reactions between Certain Trialkoxytungsten Alkylidyne Complexes and Carbon Monoxide. Competitive C–C Bond Formation Leading to Alkyne or Ketenyl Complexes

Malcolm H. Chisholm,* Douglas Ho, John C. Huffman, and Nancy S. Marchant

Department of Chemistry and Molecular Structure Center, Indiana University, Bloomington, Indiana 47405

Received August 22, 1988

Carbonylation of hydrocarbon solutions of $[(t\text{-BuO})_3W{\equiv}CMe]_2$ (1 atm, 22 °C) leads to the formation of $W_2(O\text{-}t\text{-Bu})_6(\mu\text{-}C_2Me_2)(CO)$ (I) which has been isolated as a dark blue crystalline compound. In the solid state I adopts a molecular structure based on the fusing of two trigonal bipyramids along a common axial (μ-O-*t*-Bu) and equatorial (μ-C_2Me_2) edge. A crosswise bridged alkyne, C–C = 1.36 (2) Å, spans a W–W bond of distance of 2.633 (1) Å. The NMR data are consistent with the maintenance of the same type of structure in solution. The W–CO moiety shows ν(CO) = 1917 cm^{-1} and in the ^{13}C NMR spectrum, δ 220.7 ppm with $J_{^{183}W-^{13}C}$ = 221 Hz. Under similar experimental conditions carbonylation of $[(t\text{-BuO})_3W{\equiv}CNMe_2]_2$ and $(i\text{-PrO})_3W(\equiv CNR_2)(py)_2$ gave $[(t\text{-BuO})_3W(Me_2NCCO)]_2$ (II) and $[py_2(i\text{-PrO})_3W(R_2NCCO)]_2$ (III) where R = Me (IIIa) and R = Et (IIIb). In compounds II and III carbonyl carbon–alkylidyne carbon bond formation has occurred leading to the formation of (dialkylamino)ketenyl ligands that act as bridging ligands, being η^2-C_2 bonded to one tungsten atom and η^1-O bonded to the other. The molecular structure of II in the solid state reveals local square-pyramidal coordination about the tungsten atoms with the η^2-C_2 moiety in the apical position. The structure of IIIb is related to II by the addition of a py ligand trans to the η^2-C_2 ligand. The central $W_2C_2O_2$ involving the μ-η^2,η^1-R_2NCCO ligands is planar, and there is evidently extensive π-delocalization within the NCCO moieties as evidenced by N–C, C–C, and C–O distances which span a range 1.32–1.33 Å. The compounds III show facile exchange with free carbon monoxide, implying that $CO\text{–}CNR_2$ bond formation is reversible in solution. Moreover, compound IIIa slowly reacts in solution to give an isomer IV that is shown to be $(\eta^2\text{-}C_2(NMe_2)_2)(i\text{-PrO})_2W(\mu\text{-O-}i\text{-Pr})_3W(O\text{-}i\text{-Pr})(CO)_2$. This compound may be viewed as a confacial bioctahedron in which the η^2-$C_2(NMe_2)_2$ and two CO ligands occupy terminal positions. The W–W distance of 3.1 Å implies the lack of any direct M–M bond, and this is understood in terms of extensive back-bonding to the η^2-alkyne and cis carbonyl ligands. The values ν(CO) = 1892 and 1758 cm^{-1} and C–W–C = 72.7 (10)° are similar to those seen in the d^4 *cis*-$Mo(CO)_2$ containing compound $Mo(O\text{-}t\text{-Bu})_2(CO)_2(py)_2$. In solution there is evidence of restricted rotation about the alkyne–C–NMe_2 bonds. Crystal data for I at −155 °C: a = 13.172 (3) Å, b = 15.471 (4) Å, c = 17.532 (5) Å, β = 101.03 (1)°, Z = 4, D_{calcd} = 1.683 g cm^{-3}, and space group $P2_1/n$. For II at −155 °C: a = 11.253 (3) Å, b = 9.881 (2) Å, c = 9.766 (3) Å, β = 71.14 (1)°, γ = 76.85 (1)°, Z = 1, D_{calcd} = 1.621 g cm^{-3}, and space group $P\bar{1}$. For IIIb at −102 °C: a = 9.992 (3) Å, b = 19.467 (8) Å, c = 13.016 (4) Å, β = 116.28 (1)°, Z = 2, D_{calcd} = 1.616 g cm^{-3}, and space group $P2_1/c$. For $W_2(O\text{-}i\text{-Pr})_6(\eta^2\text{-}C_2(NMe_2)_2)(CO)_2{\cdot}C_6D_6$ at −115 °C: a = 22.794 (6) Å, b = 15.621 (3) Å, c = 10.875 (2) Å, β = 90.09 (1)°, Z = 4, D_{calcd} = 1.661 g cm^{-3}, and space group $P2_1/a$.

Introduction

Following the discovery that the d^1–d^1 dinuclear compound $(i\text{-PrO})_4W_2(\mu\text{-}CSiMe_3)_2$ and carbon monoxide react to give cleavage of the C≡O triple bond (eq 1),[1] it was decided to investigate the reactivity of some formally d^0 $(RO)_3W{\equiv}CR'$ complexes with C≡O. Knowing that certain $(RO)_3W{\equiv}CR'$ complexes react with alkynes to give alkyne metathesis,[2] a plausible reaction involving no formal oxidation state change of the metal is shown in eq 2.

$$(i\text{-PrO})_4W_2(\mu\text{-}CSiMe_3)_2 + C{\equiv}O \rightarrow (i\text{-PrO})_3W(\mu\text{-}CSiMe_3)(\mu\text{-}CCSiMe_3)W(O)(O\text{-}i\text{-Pr}) \quad (1)$$

$$(RO)_3W{\equiv}CR' + C{\equiv}O \rightarrow (RO)_3W{-}C{\equiv}CR'(O) \quad (2)$$

Prompted by the above considerations we found that $(t\text{-BuO})_3W{\equiv}CMe$, $(t\text{-BuO})_3W{\equiv}CNMe_2$, and $(i\text{-PrO})_3W{\equiv}CNR'_2$, where R′ = Me and Et, and CO did react, but contrary to our expectations formation of an acetylide ligand did not occur in any case. However, carbon–carbon bond formation did occur in one of two modes. Preliminary reports of these studies have appeared.[3,4]

Results and Discussion

Reactions. $[(t\text{-BuO})_3W{\equiv}CMe]_2$ and CO. Crystalline samples of $[(t\text{-BuO})_3W{\equiv}CMe]_2$[5] dissolved in hydrocarbon solvents react slowly at room temperature with 1 atm of CO to give deep blue solutions. The reaction is complete after 2 days. ^1H NMR spectroscopy implicated a static compound in solution with the *tert*-butoxide ligands in an integral ratio of 2:2:1:1 and only one signal for the WCMe moiety. The data were consistent with a dimeric compound containing a mirror plane of symmetry. An infrared ν(CO) band at 1917 cm^{-1}, and a ^{13}C NMR signal at 220.7 ppm with J_{WC} = 221 Hz (^{183}W, $I = {}^1/_2$, 14.5% natural abundance) indicated a terminal C≡O ligand. The spectroscopic evidence suggested the possibility that carbyne coupling had occurred in solution, and X-ray crystallographic analysis on a solid sample confirmed that $W_2(O\text{-}t\text{-Bu})_6(\mu\text{-}C_2Me_2)(CO)$ (I) had been formed.

No similar reation was observed between $(t\text{-BuO})_3W{\equiv}CR$ compounds, where R = Et or Ph, and CO.[25]

$[(RO)_3W{\equiv}CNR']_2$ Compounds and CO. $[(t\text{-BuO})_3W{\equiv}CNMe_2]_2$[6] and $(i\text{-PrO})_3W{\equiv}CNR'_2(py)_2$, where R′ = Me and Et, were allowed to react with 1 atm of CO. For $[(t\text{-BuO})_3W{\equiv}CNMe_2]_2$ the reaction proceeded slowly over the course of 2 days at room temperature, while the

(1) Chisholm, M. H.; Heppert, J. A.; Huffman, J. C.; Streib, W. E. *J. Chem. Soc., Chem. Commun.* **1985**, 1771.
(2) Freudenberger, J. H.; Schrock, R. R.; Churchill, M. H.; Rhiengold, A. L.; Ziller, J. W. *Organometallics* **1984**, *3*, 1563.
(3) Chisholm, M. H.; Conroy, B. K.; Huffman, J. C.; N. S. Marchant *Angew. Chem., Int. Ed. Engl.* **1986**, *25*, 446.
(4) Chisholm, M. H.; Huffman, J. C.; Marchant, N. S. *J. Chem. Soc., Chem. Commun.* **1986**, 717.
(5) Chisholm, M. H.; Hoffman, D. M.; Huffman, J. C. *Inorg. Chem.* **1983**, *22*, 2903.
(6) Chisholm, M. H.; Huffman, J. C.; Marchant, N. S. *J. Am. Chem. Soc.* **1983**, *105*, 6162.

0276-7333/89/2308-1626$01.50/0

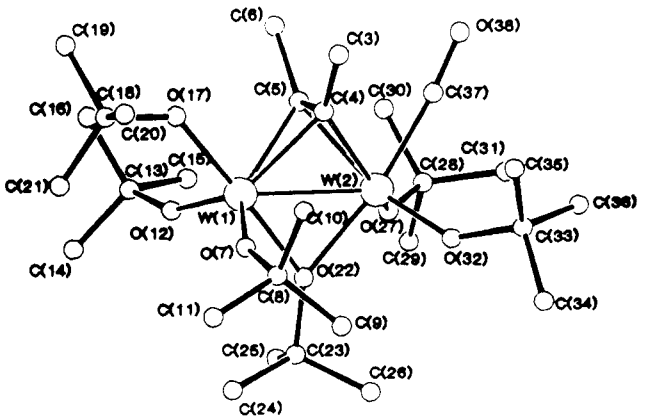

Figure 1. A ball-and-stick drawing of the $W_2(O\text{-}t\text{-}Bu)_6(\mu\text{-}C_2Me_2)(CO)$ molecule.

Table I. Pertinent Bond Distances (Å) for $W_2(O\text{-}t\text{-}Bu)_6(\mu\text{-}C_2Me_2)(CO)$ Using the Numbering Scheme Shown in Figure 1

A	B	dist
W(1)	W(2)	2.6326 (10)
W(1)	O(7)	1.890 (10)
W(1)	O(12)	1.876 (9)
W(1)	O(17)	1.968 (10)
W(1)	O(22)	2.065 (10)
W(1)	C(4)	2.124 (15)
W(1)	C(5)	2.169 (16)
W(2)	O(22)	2.064 (9)
W(2)	O(27)	1.922 (10)
W(2)	O(32)	1.923 (10)
W(2)	C(4)	2.173 (14)
W(2)	C(5)	2.098 (15)
W(2)	C(37)	1.998 (15)
O(7)	C(8)	1.465 (17)
O(12)	C(13)	1.451 (17)
O(17)	C(18)	1.437 (19)
O(22)	C(23)	1.443 (17)
O(27)	C(28)	1.416 (18)
O(32)	C(33)	1.426 (16)
O(38)	C(37)	1.159 (17)
C(3)	C(4)	1.491 (22)
C(4)	C(5)	1.361 (22)
C(5)	C(6)	1.520 (23)

isopropoxide complexes reacted at −15 °C within 12 h to form red solutions. The reactions employing $[(t\text{-}BuO)_3W{\equiv}CNMe_2]_2$ and $(i\text{-}PrO)_3W{\equiv}CNEt_2(py)_2$ gave red crystals from concentrated hexane solutions. It was found that C–C bond formation had also occurred in these cases; however, under these conditions CO had inserted into the metal–carbyne bond to form a η^2-ketenyl ligand,[7] i.e. forming $[(t\text{-}BuO)_3W(Me_2NCCO)]_2$ (II) and $[(i\text{-}PrO)_3W(R'_2NCCO)py]_2$ (III), where R′ = Me (a) and Et (b). As described later IIIa isomerizes to IV in solution.

Solid-State and Molecular Structures. $W_2(O\text{-}t\text{-}Bu)_6(\mu\text{-}C_2Me_2)(CO)$. Figure 1 shows a ball and stick diagram of compound I. I may be viewed as two trigonal bipyramids joined via axial (μ-O-*t*-Bu) and equatorial (μ-C_2Me_2) ligands. Tables I and II contain pertinent bond distances and angles of I, respectively. A series of $W_2(OR)_6(\mu\text{-}C_2R_2)L_x$ complexes have been synthesized,[8] and $W_2(O\text{-}t\text{-}Bu)_6(\mu\text{-}C_2H_2)(py)$[9] is related to I by the substitution

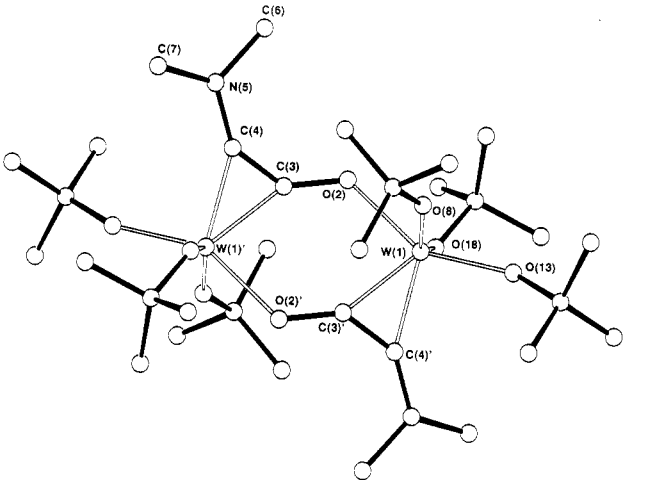

Figure 2. A ball-and-stick drawing of the $[(t\text{-}BuO)_3W(Me_2NCCO)]_2$ molecule.

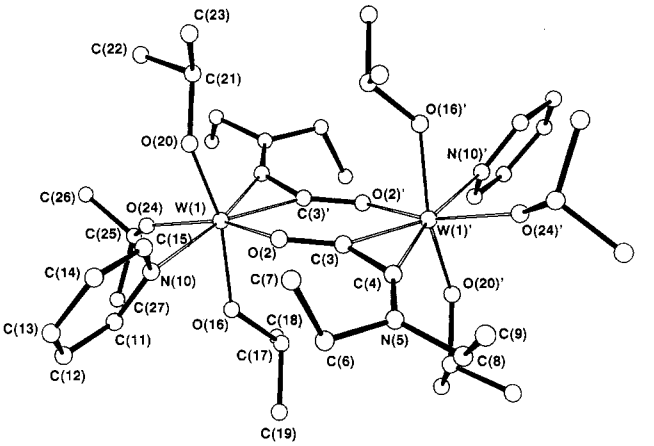

Figure 3. A ball-and-stick drawing of the $[(i\text{-}PrO)_3W(\mu\text{-}Et_2NCCO)(py)]_2$ molecule.

of py for CO. It is very interesting to note that the μ-C–C distance in I is shorter than that in $W_2(O\text{-}t\text{-}Bu)_6(\mu\text{-}C_2H_2)(py)$ (1.361 (22) Å vs 1.441 (14) Å, respectively). Also the W–W distance is shorter (2.6326 (10) Å vs 2.665 (1) Å) indicating that the dimethylacetylene in I is less reduced that the acetylene in the pyridine adduct. Both compounds show comparable W–O-*t*-Bu bond lengths so that the difference between the compounds may be attributed to the ancillary ligand (L = CO or py).

$[(RO)_3W(R'_2NCCO)]_2$ Complexes. The molecular structure of II is shown in Figure 2 and reveals the formation of a η^2-bridging ketenyl ligand by carbonyl carbyne coupling. The local coordination geometry about each W atom may be viewed as square pyramidal with the η^2-C_2 moiety occupying the apical position. The ketenyl O atom has a dative bond into the equatorial plane of each W atom and forms a planar six-membered ring of the formula $W_2C_2O_2$. The structure of IIIb is analogous to II with the addition of a py ligand trans to the apical η^2-C_2 unit as shown in Figure 3. Pertinent bond distances and angles for $[(t\text{-}BuO)_3W(Me_2NCCO)]_2$ are given in Tables III and IV while Tables V and VI have the bond distances and angles for compound IIIb.

The two compounds show very similar bond lengths and angles with the average W–OR bond lengths being 1.91 Å for II and 1.93 Å for IIIb. Compound IIIb has an addi-

(7) η^2-Ketenyl ligands are now well-known and are generally formed from the C–C coupling of carbonyl and carbyne (or alkylidene) ligands. See: Mayr, A.; McDermott, G. A.; Dorries, A. M.; Van Engen, D. *Organometallics* **1987**, *6*, 1503, and for listings of other examples, ref 6–9 cited therein.

(8) For a recent review see: Chisholm, M. H.; Conroy, B. K.; Eichhorn, B. W.; Folting, K.; Hoffman, D. M.; Huffman, J. C.; Marchant, N. S. *Polyhedron* **1987**, *6*, 783.

(9) Chisholm, M. H.; Folting, K.; Hoffman, D. M.; Huffman, J. C. *J. Am. Chem. Soc.* **1984**, *106*, 6794.

Table II. Pertinent Bond Angles (deg) for $W_2(O\text{-}t\text{-}Bu)_6(\mu\text{-}C_2Me_2)(CO)$ Using the Numbering Scheme Found in Figure 1

A	B	C	angle
W(2)	W(1)	O(7)	107.8 (3)
W(2)	W(1)	O(12)	108.4 (3)
W(2)	W(1)	O(17)	132.0 (3)
W(2)	W(1)	O(22)	50.38 (25)
W(2)	W(1)	C(4)	53.1 (4)
W(2)	W(1)	C(5)	50.7 (4)
O(7)	W(1)	O(12)	125.7 (4)
O(7)	W(1)	O(17)	92.7 (4)
O(7)	W(1)	O(22)	86.9 (4)
O(7)	W(1)	C(4)	100.7 (6)
O(7)	W(1)	C(5)	137.6 (5)
O(12)	W(1)	O(17)	92.0 (4)
O(12)	W(1)	O(22)	86.2 (4)
O(12)	W(1)	C(4)	133.4 (5)
O(12)	W(1)	C(5)	96.8 (5)
O(17)	W(1)	O(22)	177.5 (4)
O(17)	W(1)	C(4)	81.1 (5)
O(17)	W(1)	C(5)	84.8 (5)
O(22)	W(1)	C(4)	101.4 (5)
O(22)	W(1)	C(5)	97.1 (5)
C(4)	W(1)	C(5)	37.0 (6)
W(1)	W(2)	O(22)	50.39 (27)
W(1)	W(2)	O(27)	118.18 (28)
W(1)	W(2)	O(32)	114.0 (3)
W(1)	W(2)	C(4)	51.4 (4)
W(1)	W(2)	C(5)	53.1 (4)
W(1)	W(2)	C(37)	120.2 (5)
O(22)	W(2)	O(27)	89.8 (4)
O(22)	W(2)	O(32)	91.8 (4)
O(22)	W(2)	C(4)	99.7 (5)
O(22)	W(2)	C(5)	99.3 (5)
O(22)	W(2)	C(37)	170.5 (5)
O(27)	W(2)	O(32)	111.9 (4)
O(27)	W(2)	C(4)	142.3 (5)
O(27)	W(2)	C(5)	105.5 (5)
O(27)	W(2)	C(37)	94.8 (5)
O(32)	W(2)	C(4)	104.2 (5)
O(32)	W(2)	C(5)	140.9 (5)
O(32)	W(2)	C(37)	94.1 (5)
C(4)	W(2)	C(5)	37.1 (6)
C(4)	W(2)	C(37)	71.6 (6)
C(5)	W(2)	C(37)	71.5 (6)
W(1)	O(7)	C(8)	158.2 (9)
W(1)	O(12)	C(13)	153.8 (10)
W(1)	O(17)	C(18)	134.0 (9)
W(1)	O(22)	W(2)	79.2 (3)
W(1)	O(22)	C(23)	139.7 (8)
W(2)	O(22)	C(23)	140.5 (9)
W(2)	O(27)	C(28)	140.7 (9)
W(2)	O(32)	C(33)	142.5 (9)
W(1)	C(4)	W(2)	75.6 (5)
W(1)	C(4)	C(3)	135.0 (11)
W(1)	C(4)	C(5)	73.3 (9)
W(2)	C(4)	C(3)	144.0 (11)
W(2)	C(4)	C(5)	68.5 (9)
C(3)	C(4)	C(5)	130.4 (15)
W(1)	C(5)	W(2)	76.2 (5)
W(1)	C(5)	C(4)	69.7 (9)
W(1)	C(5)	C(6)	134.5 (11)
W(2)	C(5)	C(4)	74.4 (9)
W(2)	C(5)	C(6)	145.1 (12)
C(4)	C(5)	C(6)	126.2 (14)

tional dative bond involving the py ligand with a W–py bond length of 2.364 (8) Å which may account for the slightly longer W–O bonds in IIIb. The ketenyl ligand is planar, as is the $W_2C_2O_2$ ring indicating that there is an extensive π system joining the ketenyl ligands and the W atoms. The π system within the ketenyl ligand is seen in the N–C, C–C, and C–O bond lengths which are all characteristic of partial double-bond character being 1.32 Å for C–O and 1.33 Å for the C–C and C–N in II. The structures may be compared to other compounds with η^2-ketenyl

Table III. Pertinent Bond Distances (Å) for $[(t\text{-}BuO)_3W(Me_2NCCO)]_2$ Using the Numbering Scheme Found in Figure 2

A	B	dist
W(1)	O(2)	2.092 (6)
W(1)	O(8)	1.883 (6)
W(1)	O(13)	1.931 (5)
W(1)	O(18)	1.919 (6)
W(1)	C(3)	2.001 (8)
W(1)	C(4)	2.024 (8)
O(2)	C(3)	1.321 (10)
O(8)	C(9)	1.449 (10)
O(13)	C(14)	1.457 (10)
O(18)	C(19)	1.431 (10)
N(5)	C(4)	1.327 (11)
N(5)	C(6)	1.456 (12)
N(5)	C(7)	1.462 (12)
C(3)	C(4)	1.325 (12)
C(9)	C(10)	1.525 (13)
C(9)	C(11)	1.509 (14)
C(9)	C(12)	1.509 (15)
C(14)	C(15)	1.534 (13)
C(14)	C(16)	1.503 (14)
C(14)	C(17)	1.510 (14)
C(19)	C(20)	1.536 (13)
C(19)	C(21)	1.510 (14)
C(19)	C(22)	1.523 (13)

Table IV. Pertinent Bond Angles (deg) for $[(t\text{-}BuO)_3W(Me_2NCCO)]_2$ Using the Numbering Scheme Found in Figure 2

A	B	C	angle
O(2)	W(1)	O(8)	84.05 (24)
O(2)	W(1)	O(13)	148.73 (24)
O(2)	W(1)	O(18)	82.05 (23)
O(2)	W(1)	C(3)	83.3 (3)
O(2)	W(1)	C(4)	117.62 (28)
O(8)	W(1)	O(13)	89.16 (24)
O(8)	W(1)	O(18)	147.56 (25)
O(8)	W(1)	C(3)	99.38 (27)
O(8)	W(1)	C(4)	117.6 (3)
O(13)	W(1)	O(18)	87.75 (24)
O(13)	W(1)	C(3)	127.9 (3)
O(13)	W(1)	C(4)	92.6 (3)
O(18)	W(1)	C(3)	107.88 (27)
O(18)	W(1)	C(4)	94.8 (3)
C(3)	W(1)	C(4)	38.4 (3)
W(1)	O(2)	C(3)	125.9 (5)
W(1)	O(8)	C(9)	150.7 (5)
W(1)	O(13)	C(14)	142.1 (5)
W(1)	O(18)	C(19)	129.0 (5)
C(4)	N(5)	C(6)	119.2 (7)
C(4)	N(5)	C(7)	121.3 (8)
C(6)	N(5)	C(7)	116.5 (8)
W(1)	C(3)	O(2)	148.9 (6)
W(1)	C(3)	C(4)	71.8 (5)
O(2)	C(3)	C(4)	139.0 (8)
W(1)	C(4)	N(5)	147.8 (7)
W(1)	C(4)	C(3)	69.8 (5)
N(5)	C(4)	C(3)	142.2 (8)
O(8)	C(9)	C(10)	105.8 (7)
O(8)	C(9)	C(11)	109.2 (7)
O(8)	C(9)	C(12)	108.8 (8)
C(10)	C(9)	C(11)	110.8 (9)
C(10)	C(9)	C(12)	109.9 (9)
C(11)	C(9)	C(12)	112.2 (10)
O(13)	C(14)	C(15)	105.9 (7)
O(13)	C(14)	C(16)	112.0 (7)
O(13)	C(14)	C(17)	106.8 (8)
C(15)	C(14)	C(16)	110.4 (8)
C(15)	C(14)	C(17)	109.3 (8)
C(16)	C(14)	C(17)	112.1 (9)
O(18)	C(19)	C(20)	107.5 (7)
O(18)	C(19)	C(21)	110.6 (7)
O(18)	C(19)	C(22)	106.8 (7)
C(20)	C(19)	C(21)	111.6 (9)
C(20)	C(19)	C(22)	109.0 (8)
C(21)	C(19)	C(22)	111.1 (9)

Table V. Pertinent Bond Distances (Å) for $[(i\text{-PrO})_3W(Et_2NCCO)(py)]_2$ Using the Numbering Scheme Found in Figure 3

A	B	dist
W(1)	O(2)	2.104 (7)
W(1)	O(16)	1.933 (8)
W(1)	O(20)	1.923 (8)
W(1)	O(24)	1.952 (7)
W(1)	N(10)	2.364 (8)
W(1)	C(3)	2.003 (11)
W(1)	C(4)	2.074 (11)
O(2)	C(3)	1.297 (13)
O(16)	C(17)	1.434 (13)
O(20)	C(21)	1.437 (14)
O(24)	C(25)	1.394 (14)
N(5)	C(4)	1.332 (14)
N(5)	C(6)	1.463 (15)
N(5)	C(8)	1.464 (14)
N(10)	C(11)	1.313 (15)
N(10)	C(15)	1.325 (15)
C(3)	C(4)	1.353 (15)
C(6)	C(7)	1.514 (20)
C(8)	C(9)	1.500 (20)
C(11)	C(12)	1.426 (17)
C(12)	C(13)	1.342 (20)
C(13)	C(14)	1.391 (20)
C(14)	C(15)	1.393 (17)
C(17)	C(18)	1.529 (20)
C(17)	C(19)	1.496 (18)
C(21)	C(22)	1.494 (21)
C(21)	C(23)	1.503 (20)
C(25)	C(26)	1.546 (18)
C(25)	C(27)	1.516 (20)

ligands, with and without dative-type bonds from the O atom.[10] The C=O and C=C distances of 1.32 and 1.32 Å are similar to the other complexes listed in Table VII as are the W–C distances of 2.03 and 2.00 Å.

The structures of II and IIIb also have striking resemblance to the structures of $W_4(CO)_2(O\text{-}i\text{-}Pr)_{12}(py)_2$ and $W_4(CO)_2(O\text{-}i\text{-}Pr)_{12}$ which also have $W_2C_2O_2$ six-membered rings as shown below.[11,12]

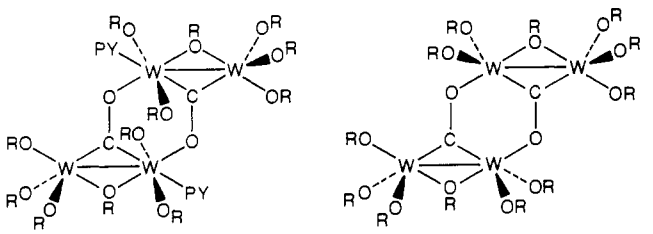

The relationship between the compounds may be recognized in Hoffmann's isolobal analogies between organic fragments and metal fragments.[11] The $(RO)_3M$ fragment is islobal to the $(R_2N)C$ fragment. Therefore, one might expect that similarities would exist in the bonding in compounds containing these fragments. In fact the C=O and C=O—W bond distances are comparable being 1.321 (10) and 2.092 (6) Å for II and 1.352 (13) and 1.974 (8) Å for $W_4(CO)_2(O\text{-}i\text{-}Pr)_{12}$. The $W_2C_2O_2$ ring in $W_4(CO)_2(O\text{-}i\text{-}Pr)_{12}$ has been compared to that for benzene, and Fenske–Hall calculations have shown that there is an extensive π system which involves the d orbitals of the metal atoms.[14] An analogous π system may be invoked for II and IIIb.

(10) Birdwhistell, K. R.; Tonker, T. L.; Templeton, J. L. *J. Am. Chem. Soc.* **1985**, *107*, 4474. See also ref 7.
(11) Cotton, F. A.; Schwotzer, W. J. *J. Am. Chem. Soc.* **1983**, *105*, 4955.
(12) Chisholm, M. H.; Hoffman, D. M.; Huffman, J. C. *Organometallics* **1985**, *4*, 986.
(13) Hoffmann, R. *Angew. Chem., Int. Ed. Engl.* **1981**, *21*, 711.
(14) Blower, P. J.; Chisholm, M. H.; Clark, D. L.; Eichhorn, B. W. *Organometallics* **1986**, *5*, 2125.

Table VI. Pertinent Bond Angles (deg) for $[(i\text{-PrO})_3W(Et_2NCCO)(py)]_2$ Using the Numbering Scheme Found in Figure 3

A	B	C	angle
O(2)	W(1)	O(16)	86.4 (3)
O(2)	W(1)	O(20)	85.7 (3)
O(2)	W(1)	O(24)	153.5 (3)
O(2)	W(1)	N(10)	73.1 (3)
O(2)	W(1)	C(3)	79.1 (3)
O(2)	W(1)	C(4)	115.9 (4)
O(16)	W(1)	O(20)	157.4 (3)
O(16)	W(1)	O(24)	86.4 (3)
O(16)	W(1)	N(10)	78.7 (3)
O(16)	W(1)	C(3)	93.0 (4)
O(16)	W(1)	C(4)	106.0 (4)
O(20)	W(1)	O(24)	91.2 (3)
O(20)	W(1)	N(10)	78.7 (3)
O(20)	W(1)	C(3)	106.3 (4)
O(20)	W(1)	C(4)	96.6 (4)
O(24)	W(1)	N(10)	80.4 (3)
O(24)	W(1)	C(3)	126.8 (4)
O(24)	W(1)	C(4)	90.6 (4)
N(10)	W(1)	C(3)	151.4 (4)
N(10)	W(1)	C(4)	169.7 (4)
C(3)	W(1)	C(4)	38.7 (4)
W(1)	O(2)	C(3)	130.2 (7)
W(1)	O(16)	C(17)	133.0 (7)
W(1)	O(20)	C(21)	137.2 (7)
W(1)	O(24)	C(25)	137.7 (7)
C(4)	N(5)	C(6)	118.0 (10)
C(4)	N(5)	C(8)	123.7 (9)
C(6)	N(5)	C(8)	118.2 (9)
W(1)	N(10)	C(11)	120.6 (8)
W(1)	N(10)	C(15)	120.6 (8)
C(11)	N(10)	C(15)	118.8 (10)
W(1)	C(3)	O(2)	148.1 (8)
W(1)	C(3)	C(4)	73.5 (6)
O(2)	C(3)	C(4)	138.4 (10)
W(1)	C(4)	N(5)	158.2 (8)
W(1)	C(4)	C(3)	67.8 (6)
N(5)	C(4)	C(3)	133.9 (10)
N(5)	C(6)	C(7)	113.3 (11)
N(5)	C(8)	C(9)	112.8 (12)
N(10)	C(11)	C(12)	122.8 (13)
C(11)	C(12)	C(13)	117.9 (14)
C(12)	C(13)	C(14)	119.7 (13)
C(13)	C(14)	C(15)	118.6 (13)
N(10)	C(15)	C(14)	122.2 (13)
O(16)	C(17)	C(18)	109.6 (11)
O(16)	C(17)	C(19)	108.8 (9)
C(18)	C(17)	C(19)	111.8 (13)
O(20)	C(21)	C(22)	109.9 (12)
O(20)	C(21)	C(23)	108.2 (13)
C(22)	C(21)	C(23)	111.8 (13)

NMR and Solution Studies. II is not fluxional on the NMR time scale in toluene-d_8 at room temperature. The ^1H NMR spectrum shows a 2:1 pattern for the *tert*-butoxide methyl signals while there is a 1:1 pattern for the proximal and distal methyls of the ketenyl ligand showing that there is restricted rotation about the $C\text{–}NMe_2$ bond. II*, prepared from reaction with ^{13}C-labeled CO, shows an enhanced signal at 241 ppm in the ^{13}C NMR spectrum with coupling to inequivalent ^{183}W nuclei of 28 and 9 Hz indicating that the dimeric structure is maintained in solution.

Compounds IIIa and IIIb show much more interesting solution behavior. Room-temperature ^1H NMR spectra show only one type of alkoxide and equivalent R'_2N groups. ^{13}C NMR spectra at room temperature with ^{13}C-labeled CO compounds III* show a signal at 242 ppm for IIIa and 236 ppm for IIIb. No tungsten coupling could be seen in the spectra. Both compounds show a signal at 184 ppm indicating that there is free ^{13}CO in solution. Even starting with crystalline samples, free CO is found in solution. A crossover experiment with unlabeled IIIa and added free

Table VII. Pertinent Structural Features of η^2-Ketenyl Complexes of W

compound[a]	W–C_b	W–C_a	C_a–C_b	C_a–O	C_b–R	ref
(Cp)(PMe_3)(CO)W(η^2-OCCC$_6$H$_4$Me)	1.97	2.07	1.32	1.30	1.52	b
[(Cp)(PMe_3)(CO)W(η^2-HOC≡CC$_6$H$_4$Me)]$^+$	2.06	2.00	1.37	1.33	1.44	c
(detc)(dppe)(CO)W(η^2-OCCCH$_2$Ph)	2.00	2.18	1.32	1.26	1.48	10
[$(CN)_2$(phen)(CO)W(η^2-OCCPh)]$^-$	1.97	2.14	1.41	1.25		d
(PMe_3)Cl(CO)W(η^2-$AlCl_3$OCCH)	2.01	2.03	1.31	1.31		27
[(*t*-BuO)$_3$W(η^2,η^1-OCCNMe$_2$)]$_2$	2.02	2.00	1.32	1.32	1.33	this work
[(*i*-PrO)$_3$W(η^2,η^1-OCCNEt$_2$)(py)]$_2$	2.07	2.00	1.35	1.30	1.33	this work

[a] The carbon atoms of the ketenyl ligand are labeled:

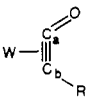

[b] Kreissl, F. R.; Friedrich, P.; Huttner, G. *Angew. Chem., Int. Ed. Engl.* **1977**, *16*, 102. [c] Jeffery, J. C.; Laurie, J. C. U.; Moore, I.; Stone, F. G. A. *J. Organomet. Chem.* **1983**, *258*, C37. [d] Fischer, E. O.; Filippou, A. C.; Alt, H. G.; Ackermann, K. *J. Organomet. Chem.* **1983**, *254*, C21.

^{13}CO shows that ^{13}CO is incorporated into IIIa at room temperature after 1 day. This indicates that formation of the ketenyl ligand is reversible at room temperature, and there is some form of equilibrium between bound and free CO.

IIIb shows only an equilibrium between free and bound CO, and no further reaction takes place for that compound. However, concomitant with incorporation of free ^{13}CO into IIIa is the slow formation of a new compound. IIIa eventually proceeds to give a single compound in high yield by ^{1}H NMR spectroscopy via several intermediates. These intermediates are evident from a plethora of ^{13}CO resonances in the ^{13}C NMR spectra and Me_2NC resonances in the ^{1}H NMR spectra.

The final compound IV, an isomer of IIIa, is fluxional on the proton NMR time scale at room temperature. Upon lowering the temperature to −60 °C a 2:2:1:1 pattern is seen for the isopropoxide ligands with those of double intensity having diastereotopic methyl resonances. Four signals are seen for Me_2NC ligands that broaden and coalesce to one signal upon warming. One ^{13}CO resonance was found in the ^{13}C NMR spectrum at 268.5 ppm with a J_{WC} of 189 Hz indicating a terminal CO. This signal did not change with temperature. The presence of two CO ligands was indicated by infrared spectroscopy due to two ν(CO) stretching bands at 1892 and 1756 cm^{-1} (ν(^{13}CO) = 1848 and 1729 cm^{-1}). The intensities of the bands indicated that the CO ligands were cis and had a bond angle of 90° or less.[15] The infrared spectra also showed bands at 1701 and 1690 cm^{-1} which may be associated with a R_2NC≡CNR_2 moiety.

The spectroscopic evidence supports the view that a dimeric compound with a mirror plane of symmetry and cis equivalent terminal CO ligands was formed. The evidence also supports the formation of a dimethylamino-substituted alkyne having restricted rotation about the C–NMe_2 bonds and restricted rotation about the C_2–W vector at low temperature. All of this is consistent with a confacial bioctahedral dimer of the formula W$_2$(O-*i*-Pr)$_6$(Me_2NC≡CNMe_2)(CO)$_2$ (IV) with a η^2-bound alkyne as shown below.

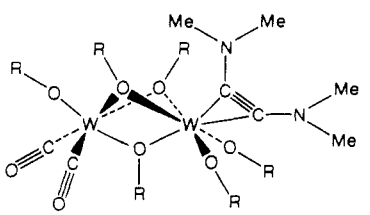

(15) Cotton, F. A.; Wilkinson, G. In *Advances Inorganic Chemistry. A Comprehensive Text*, 4th ed.; Wiley: New York, 1982; pp 1073–1076.

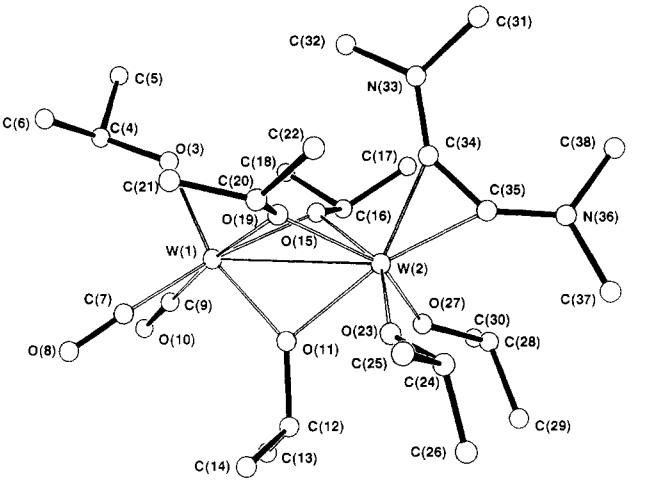

Figure 4. A ball-and-stick drawing of the W$_2$(O-*i*-Pr)$_6$(CO)$_2$(η^2-C_2(NMe_2)$_2$) molecule.

Repeated crystallizations of this compound from hexane and toluene gave flat plates unsuitable for crystallography. Fortuitously, crystals were found to grow in benzene-d_6 while attempting to recovery a ^{13}CO-labeled sample. The proposed structure was confirmed for the labeled compound W$_2$(O-*i*-Pr)$_6$(Me_2NC≡CNMe_2)(^{13}CO)$_2$·C_6D_6.

Solid-State and Molecular Structure of W$_2$(O-*i*-Pr)$_6$(C_2(NMe_2)$_2$)(CO)$_2$. Figure 4 shows a ball and stick drawing of IV. As was proposed on the basis of spectroscopic data, the coordination geometry of IV may be described as a confacial bioctahedral dimer. Tables VIII and IX contain the pertinent bond distances and angles, respectively, for compound IV. The structure has certain points of particular note.

(1) The C≡C distance for the η^2-alkyne unit is 1.36 (3) Å which appears relatively long for a η^2-alkyne though the distance is not accurately determined. For comparison the η^2-C_2 bond lengths for W$_2$(O-*i*-Pr)$_6$(μ-C_4R_4)(η^2-C_2R_2), where R = H and Me, are 1.280 (17) and 1.285 (21) Å, respectively,[16] and W$_2$(O-*i*-Pr)$_4$(CH_2Ph)$_2$(η^2-C_2Me_2)$_2$ has C–C distances of 1.31 (1) Å.[17] The long C–C distance in IV is likely due to π interaction with the lone pair of the NMe_2 units. The C_2(NC_2)$_2$ unit is planar, and the alkyne C–N bond lengths are 1.33 (3) and 1.35 (3) Å indicating partial C–N double-bond character. As an alkyne the ligand C_2(NMe_2)$_2$ may interact with the metal better due to the increased nucleophilicity of the central carbon atoms. The

(16) Chisholm, M. H.; Hoffman, D. M.; Huffman, J. C. *J. Am. Chem. Soc.* **1984**, *104*, 6806.

(17) Chisholm, M. H.; Eichhorn, B. W.; Huffman, J. C. *J. Chem. Soc., Chem. Commun.* **1985**, 861.

Table VIII. Pertinent Bond Distances (Å) for $W_2(O\text{-}i\text{-}Pr)_6(C_2(NMe_2)_2)(CO)_2$ Using the Numbering Scheme Found in Figure 4

A	B	dist
W(1)	O(3)	1.903 (16)
W(1)	O(11)	2.006 (14)
W(1)	O(15)	2.181 (15)
W(1)	O(19)	2.212 (16)
W(1)	C(7)	1.929 (26)
W(1)	C(9)	1.953 (22)
W(2)	O(11)	2.190 (15)
W(2)	O(15)	2.124 (14)
W(2)	O(19)	2.115 (15)
W(2)	O(23)	1.861 (16)
W(2)	O(27)	1.869 (16)
W(2)	C(34)	2.009 (24)
W(2)	C(35)	2.059 (26)
O(3)	C(4)	1.45 (4)
O(8)	C(7)	1.17 (3)
O(10)	C(9)	1.19 (3)
O(11)	C(12)	1.47 (3)
O(15)	C(16)	1.52 (3)
O(19)	C(20)	1.43 (3)
O(23)	C(24)	1.46 (3)
O(27)	C(28)	1.45 (4)
N(33)	C(31)	1.46 (5)
N(33)	C(32)	1.41 (3)
N(33)	C(34)	1.35 (3)
N(36)	C(35)	1.33 (3)
N(36)	C(37)	1.45 (3)
N(36)	C(38)	1.42 (4)
C(4)	C(5)	1.59 (4)
C(4)	C(6)	1.38 (5)
C(12)	C(13)	1.42 (4)
C(12)	C(14)	1.48 (4)
C(16)	C(17)	1.47 (4)
C(16)	C(18)	1.55 (4)
C(20)	C(21)	1.45 (5)
C(20)	C(22)	1.41 (6)
C(24)	C(25)	1.54 (4)
C(24)	C(26)	1.41 (4)
C(28)	C(29)	1.51 (4)
C(28)	C(30)	1.56 (4)
C(34)	C(35)	1.36 (3)
C(39)	C(40)	1.32 (5)
C(39)	C(44)	1.39 (4)
C(40)	C(41)	1.42 (5)
C(41)	C(42)	1.24 (4)
C(42)	C(43)	1.45 (5)
C(43)	C(44)	1.39 (5)

delocalized π system has also been seen in a series of Mo complexes of the formula $[Mo(CNR)_4(RHNC{\equiv}CNHR)X]^+$, where X = I, and Br.[18,19] The average C≡C distance is 1.35 Å, the C—N distance 1.32 Å, and the alkyne unit is planar. Templeton and co-workers showed that monoaminoalkynes provided increased π perpendicular electron density to a metal center relative to dialkylalkynes.[20] It is easy to extend this argument to diaminoalkynes, which should show even more enhanced donor abilities.

(2) The C–W–C angle between the cis CO ligands is small, being 72.7 (10)°, and comparable to $Mo(O\text{-}t\text{-}Bu)_2(CO)_2(py)_2$ which also has a C–M–C angle of 72°.[21] The M—C and C≡O distances are within 3σ of $Mo(O\text{-}t\text{-}Bu)_2(CO)_2(py)_2$ being 1.94 (av) and 1.18 Å (av) for IV and 1.94 and 1.16 Å (av) for $Mo(O\text{-}t\text{-}Bu)_2(CO)_2(py)_2$. These bond distances and angles point to the ability of the metal center to back bond to the carbonyl ligands. As has been pointed out many times π donor ligands raise the energy of the metal based orbitals and increase their ability to back bond to π accepting ligands.[14,21] The increased π back-bonding is also seen in the ν(CO) stretching frequencies of 1892 and 1758 cm^{-1} which may be considered very low for terminal carbonyl ligands in neutral complexes.[22]

(3) The W–W distance of 3.1 Å is approaching a typical a nonbonding distance within dimeric W alkoxide chemistry.[23] The bonding in confacial bioctahedral compounds has been discussed at length as to whether or not a compound is considered to have metal–metal interaction. One factor that has been considered is the M–L–M angle of the bridging ligands. For a bonding situation the angle should be 70.5° or smaller. In a repulsive situation between the metal centers the angle should be larger. The M–O–M angles for IV average 94° so that again it appears that a nonbonding situation prevails.

What is unusual is that the molecule may be considered to contain a M_2^{8+} core if the alkyne is viewed as a 2– ligand. It now becomes interesting to see what has happened to the metal based electrons if they are not involved in metal-metal bonding. On the basis of the bond lengths of the three bridging alkoxide ligands, the charge may be distributed between the metals to form a d^4–d^0 dimer if W(1) is considered to have two uninegative alkoxide ligands (one terminal and one bridging). W(2) has two terminal alkoxides, two bridging alkoxide ligands, and the 2-alkyne ligand leaving a d^0 metal. In the past this type of situation has still lead to some form of dative donation from the electron-rich metal center to the electron-poor metal center creating a metal–metal bond. For example, $W_2(O\text{-}i\text{-}Pr)_6(\mu\text{-}C_4Me_4)(\eta^2\text{-}C_2Me_2)$ has this same type of geometry and is felt to contain a metal–metal dative bond.[16]

It is very easy to note that W(1), which is considered a d^4 center, has two π-accepting CO ligands. These interact with the filled metal d orbitals. As the CO ligands show very strong interaction with the metal center, based on the spectroscopic and structural data, it is expected that all four metal d electrons are involved in backbonding to the cis carbonyl ligands in preference to M–M bonding.

Conclusions

It has been shown that $(RO)_3W{\equiv}CR'$ complexes react with C≡O in a manner which, while not originally anticipated, is certainly interesting. $[(t\text{-}BuO)_3W{\equiv}CMe]_2$ and $(i\text{-}PrO)_3W{\equiv}CNMe_2(py)_2$ both give thermodynamic products in which carbyne ligands have coupled to give alkyne adducts. It is proposed that CO acts a trapping agent for $W_2(O\text{-}t\text{-}Bu)_6(\mu\text{-}C_2Me_2)$. Evidence for the existence of an equilibrium between certain alkyne adducts of $W_2(OR)_6$ compounds and alkylidyne compounds $(RO)_3W{\equiv}CR'$ has been recently reviewed.[8] As a π-acid ancillary ligand, it stabilizes the alkyne adduct. In the case of $W_2(O\text{-}i\text{-}Pr)_6(CO)_2(C_2(NMe_2)_2)$ the alkyne ligand may also be trapped by the coordination of a CO ligand. The alkyne ligand moves from a bridging position to a terminal position, presumably because the latter is stabilized by the greater electron-donating ability of $(Me_2N)_2C_2$ relative to Me_2C_2. This alkyne migration generates an open coordination site which is then filled by uptake of another CO ligand.

(18) Corfield, P. W. R.; Baltasis, L. M.; Lippard, S. J. *Inorg. Chem.* **1981**, *20*, 922.
(19) Laim, C.; Corfield, P. W. R.; Lippard, S. J. *J. Am. Chem. Soc.* **1977**, *99*, 617.
(20) Templeton, J. L.; Herrick, R. S.; Morrow, J. R. *Organometallics* **1984**, *3*, 535.
(21) Chisholm, M. H.; Huffman, J. C.; Kelly, R. L. *J. Am. Chem. Soc.* **1984**, *3*, 535.
(22) See ref 15, pp 1070–1072.
(23) Chisholm, M. H. *Polyhedron* **1983**, *2*, 681.
(24) Summerville, R. H.; Hoffman, R. *J. Am. Chem. Soc.* **1979**, *101*, 3821.

Table IX. Pertinent Bond Angles (deg) for $W_2(O\text{-}i\text{-}Pr)_6(C_2(NMe_2)_2(CO)_2$ Using the Numbering Scheme Found in Figure 4

A	B	C	angle	A	B	C	angle
O(3)	W(1)	O(11)	158.9 (7)	W(1)	O(19)	W(2)	93.5 (6)
O(3)	W(1)	O(15)	90.6 (6)	W(1)	O(19)	C(20)	130.7 (15)
O(3)	W(1)	O(19)	87.6 (6)	W(2)	O(19)	C(20)	127.0 (15)
O(3)	W(1)	C(7)	96.9 (9)	W(2)	O(23)	C(24)	146.5 (15)
O(3)	W(1)	C(9)	98.6 (8)	W(2)	O(27)	C(28)	144.3 (18)
O(11)	W(1)	O(15)	75.1 (6)	C(31)	N(33)	C(32)	115.8 (24)
O(11)	W(1)	O(19)	72.7 (6)	C(31)	N(33)	C(34)	120.8 (24)
O(11)	W(1)	C(7)	96.9 (8)	C(32)	N(33)	C(34)	123.4 (22)
O(11)	W(1)	C(9)	100.7 (8)	C(35)	N(36)	C(37)	123.3 (23)
O(15)	W(1)	O(19)	67.4 (6)	C(35)	N(36)	C(38)	122.1 (23)
O(15)	W(1)	C(7)	172.0 (8)	C(37)	N(36)	C(38)	114.5 (24)
O(15)	W(1)	C(9)	109.1 (7)	O(3)	C(4)	C(5)	107.6 (24)
O(19)	W(1)	C(7)	109.9 (8)	O(3)	C(4)	C(6)	115 (3)
O(19)	W(1)	C(9)	173.0 (7)	C(5)	C(4)	C(6)	115 (3)
C(7)	W(1)	C(9)	72.7 (10)	W(1)	C(7)	O(8)	169.2 (22)
O(11)	W(2)	O(15)	72.6 (6)	W(1)	C(9)	O(10)	177.0 (20)
O(11)	W(2)	O(19)	71.1 (6)	O(11)	C(12)	C(13)	113.6 (21)
O(11)	W(2)	O(23)	81.4 (6)	O(11)	C(12)	C(14)	111.6 (21)
O(11)	W(2)	O(27)	80.3 (6)	C(13)	C(12)	C(14)	111.6 (25)
O(11)	W(2)	C(34)	153.3 (8)	O(15)	C(16)	C(17)	108.1 (21)
O(11)	W(2)	C(35)	167.5 (8)	O(15)	C(16)	C(18)	104.2 (21)
O(15)	W(2)	O(19)	70.3 (6)	C(17)	C(16)	C(18)	112.1 (25)
O(15)	W(2)	O(23)	150.6 (6)	O(19)	C(20)	C(21)	112.0 (27)
O(15)	W(2)	O(27)	88.5 (6)	O(19)	C(20)	C(22)	116 (3)
O(15)	W(2)	C(34)	86.9 (8)	C(21)	C(20)	C(22)	117 (4)
O(15)	W(2)	C(35)	116.3 (8)	O(23)	C(24)	C(25)	113.6 (20)
O(19)	W(2)	O(23)	88.7 (6)	O(23)	C(24)	C(26)	108.9 (23)
O(19)	W(2)	O(27)	148.3 (7)	C(25)	C(24)	C(26)	111.5 (24)
O(19)	W(2)	C(34)	86.1 (8)	O(27)	C(28)	C(29)	109.1 (24)
O(19)	W(2)	C(35)	119.3 (8)	O(27)	C(28)	C(30)	110.7 (24)
O(23)	W(2)	O(27)	100.7 (7)	C(29)	C(28)	C(30)	113.2 (25)
O(23)	W(2)	C(34)	112.6 (8)	W(2)	C(34)	N(33)	145.7 (18)
O(23)	W(2)	C(35)	91.6 (9)	W(2)	C(34)	C(35)	72.4 (15)
O(27)	W(2)	C(34)	116.8 (8)	N(33)	C(34)	C(35)	141.9 (24)
O(27)	W(2)	C(35)	90.9 (9)	W(2)	C(35)	N(36)	150.0 (20)
C(34)	W(2)	C(35)	39.1 (10)	W(2)	C(35)	C(34)	68.5 (14)
W(1)	O(3)	C(4)	132.9 (17)	N(36)	C(35)	C(34)	140.7 (25)
W(1)	O(11)	W(2)	97.3 (6)	C(40)	C(39)	C(44)	119 (3)
W(1)	O(11)	C(12)	137.3 (14)	C(39)	C(40)	C(41)	121 (4)
W(2)	O(11)	C(12)	125.5 (13)	C(40)	C(41)	C(42)	118 (4)
W(1)	O(15)	W(2)	94.1 (6)	C(41)	C(42)	C(43)	114 (3)
W(1)	O(15)	C(16)	127.8 (14)	C(39)	C(44)	C(43)	121 (3)
W(2)	O(15)	C(16)	122.4 (13)				

Scheme I shows the proposed reaction mechanisms.

Steric factors play an important role in these reactions because preliminary evidence suggests that $(t\text{-BuO})_3W{\equiv}CEt$ and $(t\text{-BuO})_3W{\equiv}CPh$ do not react with CO under mild conditions.[25] $(t\text{-BuO})_3W{\equiv}CNMe_2$ and $(i\text{-PrO})_3W{\equiv}CNEt_2(py)_2$ react with CO to give ketenyl complexes. However, these compounds do not react further to couple the carbyne ligands.

It has been proposed that the W≡C unit behaves as if it were polarized $W^{\delta+}$–$C^{\delta-}$, and electron-donating groups on the carbyne ligand should activate the alkylidyne complex toward acetylene metathesis.[26] This same type of reactivity is shown in these reactions with CO. We propose that the initial interaction between $(RO)_3W{\equiv}CNR'_2$ and CO is nucleophilic attack on the W atom by the CO carbon atom lone pair. This step is followed by an electrophilic interaction by the π-antibonding orbital of CO on the α carbon of the carbyne ligand. Carbon–carbon bond formation is further stabilized by interaction of the amido lone pair electrons forming an extended π system in the ketenyl ligand (R'_2NCCO). This type of stabilization is not possible in the alkyl-substituted carbyne, and the ketenyl ligand is not formed or at least not stable. Even the amido-substituted ketenyl ligands show an equilibrium between free and bound CO emphasizing the lability of this bond. Finally it should be noted that the ability of tungsten to act as a Lewis acidic center toward the ketenyl ligand has a parallel in the reaction between $W(CH)Cl(PMe_3)_4$ and CO in the presence of $AlCl_3$. Here $AlCl_3$ acts as a Lewis acid stabilizing the compound $W(Cl)(CO)(\eta^2\text{-}HC_2OAlCl_3)(PMe_3)_3$.[27]

Experimental Section

Reagents and General Techniques. General procedures and the preparation of $(t\text{-BuO})_3WCNR'_2$ and $(t\text{-BuO})_3WCMe$ have been previously described.[6,26,28] CO was purchased from Matheson and used without further purification. ^{13}CO was purchased from Monsanto Research Corp. and used without further purification. All manipulations were carried out under inert atmospheres using standard Schlenk and drybox techniques.

^1H NMR spectra were recorded on a Nicolet NT-360 or a Varian XL-300 spectrophotometer in toluene-d_8 or benzene-d_6. The ^{13}C NMR spectra were recorded on a Varian XL-300 spectrophotometer in toluene-d_8 or benzene-d_6. ^1H NMR chemical shifts are in parts per million relative to protio impurities in the solvents, namely, δ 7.15 for benzene-d_6 and δ 2.09 for toluene-d_8 methyl. ^{13}C NMR chemical shifts are in parts per million relative to the toluene-d_8 ipso carbon set at δ 137.50.

(25) Chisholm, M. H.; Conroy, B. K., results to be published.
(26) Listemann, M. L.; Schrock, R. R. *Organometallics* **1985**, *4*, 74.
(27) Churchill, M. R.; Wassermann, H. J.; Holmes, S. J.; Schrock, R. R. *Organometallics* **1982**, *1*, 766.
(28) Schrock, R. R.; Listemann, M. L.; Sturgeoff, L. G. *J. Am. Chem. Soc.* **1982**, *104*, 4291.
(29) Akiyama, M.; Chisholm, M. H.; Cotton, F. A.; Extine, M. W.; Haitko, D. A.; Little, D.; Fanwick, P. E. *Inorg. Chem.* **1979**, *18*, 2266.

Scheme I

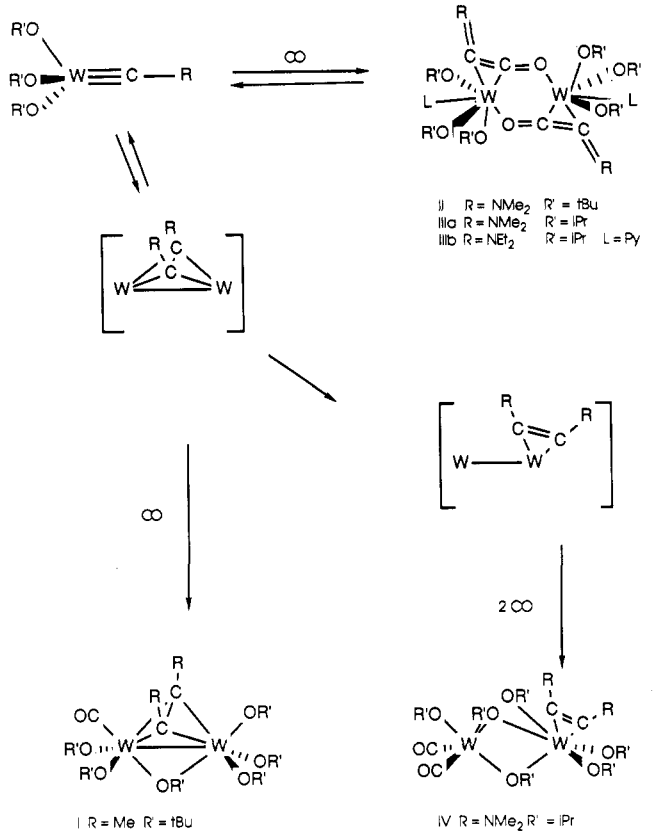

II R = NMe_2 R' = tBu
IIIa R = NMe_2 R' = iPr
IIIb R = NEt_2 R' = iPr L = Py

I R = Me R' = tBu

IV R = NMe_2 R' = iPr

$(i\text{-PrO})_3W{\equiv}CNMe_2(py)_2$. $(t\text{-BuO})_3W{\equiv}CNMe_2$ (0.250 g) was dissolved in hexane (2 mL) and py (1 mL). Excess HO-*i*-Pr (1 mL) was added via syringe and the solution stirred for 15 min. The solution volume was reduced in vacuo to 1 mL and cooled to −15 °C overnight. Red diamond-shaped crystals were isolated via filtration. IR (cm^{-1}): 1605 (w), 1579 (w), 1505 (m), 1395 (s)8 1310 (m), 1260 (w), 1216 (w), 1190 (2), 1162 (m), 1125 (vs), 1070 (w), 1045 (w), 990 (sh), 978 (s), 652 (s), 920 (m), 844 (m), 800 (w), 758 (m), 740 (w), 722 (w), 700 (m), 600 (m). ^1H NMR (benzene-d_6, room temperature): δ 8.75, 6.92, 6.63 (ortho, para, and meta protons of py), 5.5 (v br, O*CH*Me_2), 3.09 (s, *Me*$_2$NC), 1.57 (v br, OCH*Me*$_2$). Anal. Calcd: C, 45.92; H, 6.48; N, 7.30. Found: C, 45.78; H, 6.36; N, 7.24.

$(O\text{-}i\text{-Pr})_3W{\equiv}CNEt_2(py)_2$. The (diethylamino)carbyne complex was prepared in an analogous manner to that of the dimethylamino complex presented above. IR (cm^{-1}): 1602 (w), 1485 (m), 1310 (m), 1280 (w), 1218 (w), 118 (w), 1162 (m), 1122 (vs), 1072 (w), 1045 (w), 990 (s), 975 (s), 950 (s), 850 (m), 780 (w), 758 (w), 720 (w), 680 (m), 600 (m) 480 (br, w). ^1H NMR (toluene-d_8, room temperature: δ 8.74, 6.98, 6.70 (ortho, para, and meta protons of py), 5.6 (v br, O*CH*Me_2), 3.43, 1.14 (q, t, *Et*$_2$NC), 1.53 (v br, OCH*Me*$_2$).

$W_2(O\text{-}t\text{-Bu})_6(\mu\text{-}C_2Me_2)(CO)$. $[(t\text{-BuO})_3W{\equiv}CMe]_2$ (0.280 g, 0.35 mmol) was dissolved in hexane (8 mL) and frozen at liquid N_2 temperature. The flask was placed under vacuum and warmed to room temperature. One atmosphere of CO was introduced via a calibrated gas line, and the solution was stirred at room temperature for 2 days. The CO atmosphere was removed, and the solvent volume was reduced in vacuo to approximately 2 mL. The solution was cooled to −15 °C, and blue crystals formed and were filtered from the solution. IR (cm^{-1}): 1917 (s), 1265 (w), 1230 (m), 1172 (s) 985 (m), 955 (s), 935 (m), 892 (m), 780 (w, sh), 775 (w), 762 (w), 719 (w), 570 (w), 540 (w), 478 (w). ^1H NMR (toluene-d_8, room temperature): δ 3.23 (ns, C_2*Me*$_2$), 1.90, 1.44, 1.34, 1.28 (s, 1:1:2:2, O-*t*-Bu). ^{13}C NMR (toluene-d_8, room temperature): 220.7 (J_{WC} = 221 Hz).

$[W(O\text{-}t\text{-Bu})_3(Me_2NCCO)]_2$. $[(t\text{-BuO})_3WCNMe_2]_2$ (0.15 g, 0.16 mmol) was dissolved in hexane (8 mL) and frozen at liquid-nitrogen temperature. The flask was placed under vacuum and warmed to room temperature. One atmosphere of CO was introduced via a calibrated gas line, and the solution was stirred at room temperature for 2 days. The solution was concentrated in vacuo and allowed to stand at room temperature. Red crystals formed and were filtered from the solution. Anal. Calcd: C, 39.44; H, 6.82; N, 2.87. Found: C, 39.19; H, 6.67; N, 2.86. IR (cm^{-1}): 1710 (s), 1258 (w), 1230 (w), 1172 (s) 1040 (w), 1020 (w), 985 (m), 960 (s), 935 (s) 785 (m), 775 (m), 720 (m), 590 (w), 569 (m), 552 (m), 480 (m). ^1H NMR (toluene-d_8, room temperature): δ 3.28, 2.96 (s, *Me*$_2$NC), 1.50, 1.48 (s, 1:2, O-*t*-Bu). ^{13}C NMR (toluene-d_8): δ 241.7 (J_{WC} = 28, 9 Hz, Me_2NCCO).

$[W(O\text{-}i\text{-Pr})_3(Me_2NCCO)(py)]_2$. $(i\text{-PrO})_3WCNMe_2(py)_2$ (0.15 g, 0.27 mmol) was dissolved in hexane (8 mL) and frozen at liquid-nitrogen temperature. The flask was placed under vacuum and warmed to room temperature. One atmosphere of CO was introduced into the flask via a calibrated gas line. The solution was stirred at room temperature for 1 h and then cooled to −15 °C. A powdery precipitate was filtered from the solution, and the filtrate was concentrated in vacuo taking care to keep the solution cold. Anal. Calcd: C, 41.23; H, 6.15; N, 5.34. Found: C, 40.86; H, 6.21; N, 5.35. IR (cm^{-1}): 1705 (m), 1685 (m), 1320 (w), 1256 (w), 1160 (m), 1114 (s), 1030 (w), 972 (s), 838 (m), 795 (m), 750 (w), 716 (m), 682 (m), 670 (m). ^1H NMR (toluene-d_8, room temperature: δ 8.94, 7.05, 6.77 (ortho, meta, and para protons of py), 4.94 (sept, O*CH*Me_2), 3.37 (s, *Me*$_2$NC), 1.31 (d, OCH*Me*$_2$). ^{13}C NMR (toluene-d_8, room temperature): δ 242 (Me_2NCCO) 184 (CO), 150, 135, 123 (py), 74 (O*CH*Me_2) 43 (*Me*$_2$NC)8 26 (OCH*Me*$_2$).

$[W(O\text{-}i\text{-Pr})_3(Et_2NCCO)(py)]_2$. The diethylketenyl complex was prepared in an analogous manner to that of the dimethylketenyl complex but employing $(i\text{-PrO})_3WCNEt_2(py)_2$. Red crystals were isolated from the cooled solution. Anal. Calcd: C, 43.48; H, 6.58; N, 5.08. Found: C, 43.22; H, 6.41; N, 4.93. IR (cm^{-1}): 1710 (m), 1672 (m), 1600 (m), 1402 (s), 1319 (m), 1265 (s), 1210 (m), 1158 (2), 1120 (s), 1056 (w), 1032 (w), 980 (vs), 835 (m), 890 (w), 752 (w), 685 (w), 621 (w), 579 (m), 452 (w), 280 (br, w). ^1H NMR (benzene-d_6, room temperature): δ 8.81, 6.99, 6.72 (ortho, meta, and para protons of pyh), 4.93 (sept, O*CH*Me_2), 3.72, 1.17 (quart, trip, *Et*$_2$N), 1.32 (d, OCH*Me*$_2$). ^{13}C NMR (benzene-d_6, room temperature): δ 236 (Et_2NCCO), 184 (CO), 150, 135, 123 (py), 74 (O*CH*Me_2), 48 (CH_3CH_2NCCO), 25 (OCH*Me*$_2$), 15 (CH_3CH_2NCCO).

$W_2(O\text{-}i\text{-Pr})_6(\eta^2\text{-}Me_2NCCNMe_2)(CO)_2$. $(i\text{-PrO})_3WCNMe_2(py)_2$ (0.19 g, 0.35 mmol) was dissolved in hexane (8 mL) and frozen at liquid-nitrogen temperature. The flask was placed under vacuum and warmed to room temperature where 1 atm of CO was introduced into the flask. The solution was stirred for 2 days at room temperature. Upon cooling to −15 °C a red powder was obtained and filtered. Crystals suitable for X-ray crystallography were fortuitously obtained from benzene-d_6 while recovering a ^{13}C-labeled sample in an NMR tube. IR (cm^{-1}): 1892 (s) 1758 (ns), 1710 (m), 1690 (m), 1160 (m), 1119 (s), 1045 (w), 1020 (m), 975 (s), 942 (s), 842 (m), 828 (m), 770 (w), 720 (m), 635 (m), 582 (m), 460 (m, br). IR (cm^{-1}, ^{13}CO): 1848 (s), 1720 (s), 1690 (s), 1256 (m), 1160 (m), 1119 (s), 1045 (w), 1020 (m), 975 (s), 940 (s), 842 (m), 825 (s), 800 (m), 779 (w), 720 (m) 635 (m), 605 (m), 510 (m). ^1H NMR (toluene-d_8, −65 °C): δ 5.99, 5.36, 5.00, 4.18 (sept, 1:1:2:2, O*CH*Me_2), 3.86, 3.53, 2.69, 2.49 (s, 3:3:3:3, *Me*$_2$NC), 1.56, 1.51, 1.43, 1.24, 0.99 (overlapping d, OCH*Me*$_2$). ^{13}C NMR (toluene-d_8, room temperature): δ 268.5 (J_{WC} = 189 Hz, CO), 199.2, 163.0 (C_2NMe$_2$), 78 (O*CH*Me_2), 46 ((*Me*$_2$N)$_2C_2$), 28 (br, OCH*Me*$_2$), 27, 26 (OCH*Me*$_2$).

Crystallographic Studies. General operating procedures and listings of programs have been previously given.[30] A summary of crystal data is given in Table X. Atomic positional parameters for the four compounds are listed in Tables XI through XIV.

$W_2(O\text{-}t\text{-Bu})_6(\mu\text{-}C_2Me_2)(CO)$. A suitable crystal was located and transferred to the goniostat by using standard inert-atmosphere handling techniques employed by the Indiana University Molecular Structure Center (IUMSC) and cooled to −155 °C for characterization and data collection.

A systematic search of a limited hemisphere of reciprocal space located a set of diffraction maxima with monoclinic symmetry and systematic absences corresponding to the space group $P2_1/n$.

(30) Chisholm, M. H.; Folting, K.; Huffman, J. C.; Kirkpatrick, C. C. *Inorg. Chem.* **1984**, *23*, 1021.

Table X. Summary of Crystal Data[a]

	I	II	IV	IIIb
empirical formula	$W_2C_{29}O_7H_{60}$	$W_2C_{32}H_{66}O_8N_2$	$W_2C_{32}H_{60}N_2O_8$	$W_2C_4H_{72}O_8N_4$
color of crystal	black	orange	black	red-orange
cryst dimens, mm	0.16 × 0.08 × 0.12	0.20 × 0.20 × 0.22	0.08 × 0.17 × 0.16	0.15 × 0.15 × 0.20
space group	$P2_1/n$	$P\bar{1}$	$P2_1/a$	$P2_1/c$
cell dimens				
temp, °C	−155	−155	−115	−102
a, Å	13.172 (3)	11.253 (3)	22.794 (6)	9.992 (3)
b, Å	15.471 (4)	9.881 (2)	15.621 (3)	19.467 (8)
c, Å	17.532 (5)	9.766 (3)	10.875 (2)	13.016 (4)
β, deg	101.03 (1)	71.14 (1)	90.09 (1)	116.28 (1)
γ, deg		76.85 (1)		
Z, molecules/cell	4	1	4	2
V, Å^3	3506.59	998.28	3872.43	2270.39
D_{calcd}, g/cm^3	1.683	1.621	1.661	1.616
wavelength, Å	0.710 69	0.710 69	0.710 69	0.710 69
mol wt	888.49	974.58	968.53	1104.73
linear abs coeff, cm^{-1}	67.336	59.235	61.077	52.202
detector to sample dist, cm	22.5	22.5	22.5	22.5
sample to source dist, cm	23.5	23.5	23.5	23.5
av ω scan width at half height	0.25	0.25	0.25	0.25
scan speed, deg/min	4.0	4.0	4.0	4.0
scan width, deg + dispersn	2.0	2.0	2.0	2.0
individual bkgd, s	8	5	8	6
aperture size, mm	3.0 × 4.0	3.0 × 4.0	3.0 × 4.0	3.0 × 4.0
2θ range, deg	6–45	6–45	6–45	6–45
total no. of relctns collected	6617	2659	6156	3438
no. of unique intensities	4596	2622	5080	2951
no. with $F > 0.0$			4905	
no. with $F > 2.33\sigma(I)$			4201	
no. with $F > 3.00\sigma(F)$	3628	2507		2434
$R(F)$	0.0540	0.0358	0.0789	0.0452
$R_w(F)$	0.0550	0.0364	0.0885	0.0451
goodness of fit for last cycle	1.195	1.266	3.056	1.020
max δ/σ for last cycle	0.05	0.05	0.05	0.05

[a] I, W_2(O-*t*-Bu)$_6$(μ-C_2Me_2)(CO); II, [W(O-*t*-Bu)$_3$(μ-OCCNMe$_2$)]$_2$; IV, W_2(O-*i*-Pr)$_6$(C_2(NMe$_2$)$_2$)(CO)$_2$·C_6D_6; IIIb, [W(O-*i*-Pr)$_3$(py)(μ-OCCNEt$_2$)]$_2$.

Subsequent solution and refinement confirmed this choice.

The structure was solved by a combination of direct methods (MULTAN78) and Fourier techniques and refined by full-matrix least squares. There were several large peaks located in the vicinity of the two tungsten atoms, and an examination of symmetry related intensities indicated that there was a significant absorption correction. Although the crystal was cleaved from a larger crystal, the faces were approximately assigned and a correction was applied. The averaging of equivalent data improved significantly (R for averaging dropping from 0.12 to 0.08).

Many of the hydrogen atom positions were visible in a difference Fourier phased on the non-hydroen parameters. The positions of all hydrogens were calculated and placed in fixed idealized (d(C–H) = 0.95 Å) for the final cycles. The hydrogen atoms were assigned a thermal parameters of 1 + B_{iso} of the carbon atom to which they were bound.

A final difference Fourier was essentially featureless, with the largest peak being 1.70 e/Å^3, located at one of the tungstens.

[W(O-*t*-Bu)$_3$(μ-OCCNMe$_2$)]$_2$. A suitable sample was cleaved from a large single crystal and was transferred to the goniostat by using standard inert-atmosphere handling techniques employed by the IUMSC and cooled to −155 °C for characterization and data collections.

A systematic search of a limited hemisphere of reciprocal space located a set of diffraction maxima with no symmetry or systematic absences, indicating a triclinic space group. Data were collected in the usual manner by using a continuous θ–2θ scan technique. Data were reduced in the usual manner.

The structure was solved by a combination of Patterson and Fourier techniques. Hydrogen atoms were visible in a Fourier phased on the non-hydrogen parameters and were included in the final cycles. Non-hydrogen atoms were assigned anisotropic thermal parameters while hydrogens were allowed to vary isotropically. Although the crystal was larger than desirable, no absorption correction was performed due to the uneven faces. A ψ scan of two reflections near χ = 90° indicated errors due to absorption are less than 10%.

Except for four peaks of intensity 1.2–1.8 e/Å^3 located within 1 Å of the tungsten atoms, the final difference Fourier was essentially featureless, with the largest peak not associated with the metal being 0.50 e/Å^3.

[W(O-*i*-Pr)$_3$(μ-OCCNEt$_2$)(py)]$_2$. A suitable crystal was located and transferred to the goniostat by using standard inert-atmosphere handling techniques employed by the IUMSC and cooled to −102 °C for characterization and data collection. When samples were cooled to temperatures below this, a phase transition occurred which degraded significantly the quality of the diffraction. A slight thermochromism was observed upon cooling.

A systematic search of a limited hemisphere of reciprocal space located a set of diffraction maxima with monoclinic symmetry and systematic absences corresponding to the unique space group $P2_1/c$. Subsequent solution and refinement confirmed this choice. Data were collected in the usual manner by using a continuous θ–2θ scan technique. Data were reduced in the usual manner.

The structure was solved by a combination of direct methods (MULTAN78) and Fourier techniques and refined by full-matrix least squares. Hydrogen atoms were visible in a Fourier phased on the non-hydrogen parameters and were included in the final cycles. Non-hydrogen atoms were assigned anisotropic thermal parameters while hydrogens were allowed to vary isotropically.

A final difference Fourier was essentially featureless, with the largest peak being 0.50 e/Å^3.

W$_2$(O-*i*-Pr)$_6$(η^2-C$_2$(NMe$_2$)$_2$)(CO)$_2$. A suitable crystal was located and transferred to the goniostat by using standard inert-atmosphere handling techniques employed by the IUMSC and cooled to −115 °C for characterization and data collection. When cooled below this temperature, a catastrophic phase transition occurred.

A systematic search of a limited hemisphere of reciprocal space located a set of diffraction maxima with systematic absences corresponding to the unique monoclinic space group $P2_1/a$. Subsequent solution and refinement confirmed this choice. Data were collected in the usual manner by using a continuous θ–2θ scan technique. Data were reduced in the usual manner. The

Table XI. Fraction Coordinates and Isotropic Thermal Parameters for $W_2(O\text{-}t\text{-}Bu)_6(\mu\text{-}C_2Me_2)(CO)$

atom	10^4x	10^4y	10^4z	$10B_{iso}$, Å^2
W(1)	8102.2 (4)	2087.0 (4)	9207.1 (3)	12
W(2)	6835.5 (4)	2967.0 (4)	9907.7 (3)	11
C(3)	6503 (12)	3277 (11)	7903 (9)	19
C(4)	7034 (11)	3054 (11)	8708 (8)	18
C(5)	7809 (11)	3467 (10)	9198 (9)	16
C(6)	8393 (12)	4261 (11)	9007 (9)	22
O(7)	7404 (8)	1077 (7)	8785 (6)	19
C(8)	6539 (11)	528 (10)	8425 (8)	16
C(9)	5844 (12)	413 (10)	9002 (11)	24
C(10)	5969 (13)	964 (12)	7703 (10)	28
C(11)	7037 (13)	-309 (12)	8254 (11)	29
O(12)	9429 (7)	2125 (7)	9829 (5)	15
C(13)	10387 (11)	2552 (12)	10177 (10)	27
C(14)	11120 (11)	1873 (12)	10580 (10)	27
C(15)	10112 (13)	3232 (12)	10740 (10)	26
C(16)	10870 (11)	3004 (11)	9573 (9)	21
O(17)	8648 (7)	2316 (7)	8258 (6)	16
C(18)	9246 (13)	1820 (11)	7808 (9)	23
C(19)	9932 (13)	2459 (12)	7506 (10)	25
C(20)	8473 (14)	1440 (13)	7132 (11)	33
C(21)	9858 (14)	1113 (12)	8281 (10)	30
O(22)	7580 (7)	1809 (6)	10218 (6)	15
C(23)	7762 (11)	1198 (10)	10851 (8)	17
C(24)	8200 (12)	370 (12)	10585 (10)	28
C(25)	8541 (14)	1580 (12)	11547 (10)	30
C(26)	6727 (14)	1048 (12)	11103 (11)	30
O(27)	7363 (7)	3413 (6)	10930 (6)	16
C(28)	7396 (11)	4187 (11)	11364 (9)	18
C(29)	7919 (13)	3934 (11)	12206 (9)	24
C(30)	8085 (12)	4868 (11)	11062 (10)	23
C(31)	6327 (11)	4530 (11)	11353 (9)	19
O(32)	5499 (7)	2439 (6)	9840 (6)	14
C(33)	4419 (10)	2603 (11)	9606 (8)	18
C(34)	3880 (12)	1796 (12)	9803 (11)	28
C(35)	4147 (12)	3361 (11)	10062 (10)	22
C(36)	4179 (11)	2779 (12)	8745 (9)	22
C(37)	6260 (11)	4098 (10)	9474 (9)	16
O(38)	5976 (8)	4737 (7)	9159 (6)	22

Table XII. Fractional Coordinates and Isotropic Thermal Parameters for $[W(O\text{-}t\text{-}Bu)_3(\mu\text{-}OCCNMe_2)]_2$

atom	10^4x	10^4y	10^4z	$10B_{iso}$, Å^2
W(1)	3555.7 (3)	1503.5 (3)	1656.6 (3)	11
O(2)	5632 (6)	8585 (6)	603 (6)	18
C(3)	4647 (8)	-441 (8)	1414 (9)	14
C(4)	3648 (8)	-322 (9)	2623 (9)	15
N(5)	3086 (7)	-1055 (7)	3679 (8)	17
C(6)	3712 (11)	7491 (11)	3727 (12)	25
C(7)	1704 (9)	-622 (12)	4494 (12)	27
O(8)	4806 (5)	2497 (6)	1626 (6)	17
C(9)	6140 (8)	2548 (9)	1349 (10)	18
C(10)	6089 (10)	3862 (11)	2193 (12)	24
C(11)	6824 (11)	1268 (12)	1889 (15)	30
C(12)	6762 (13)	2661 (18)	-254 (13)	37
O(13)	2427 (5)	2557 (6)	3437 (6)	17
C(14)	2394 (9)	2979 (9)	4876 (9)	21
C(15)	1004 (10)	3084 (11)	5880 (11)	25
C(16)	3332 (10)	1947 (12)	5397 (11)	26
C(17)	2674 (11)	4407 (12)	4789 (13)	31
O(18)	2038 (5)	1439 (6)	1190 (6)	16
C(19)	1115 (8)	2557 (9)	896 (9)	18
C(20)	-69 (10)	2923 (14)	2280 (12)	30
C(21)	1692 (11)	3793 (12)	437 (16)	34
C(22)	722 (11)	2003 (12)	-301 (12)	27

structure was solved by a combination of direct methods (MULTAN78) and Fourier techniques and refined by full-matrix least squares. When the atoms were allowed to go anisotropic, the residuals did not decrease significantly (except for the two tungsten atoms), and in fact, several of the atoms converged to nonpositive definite thermal parameters. This indicated that the absorption correction is not well determined. The agreement between equivalent reflections (R) before and after correction for absorption decreased significantly, from 0.082 to 0.037, indicating that the correction is in the proper direction. Many of the hy-

Table XIII. Fractional Coordinates and Isotropic Thermal Parameters for $W_2(O\text{-}i\text{-}Pr)_6(\eta^2\text{-}C_2(NMe_2)_2)(CO)_2{\bullet}C_6D_6$

atom	10^4x	10^4y	10^4z	$10B_{iso}$, Å^2
W(1)	6241 (5)	2031 (1)	2489 (1)	17
W(2)	7136.1 (4)	497 (1)	2331 (1)	18
O(3)	5435 (7)	1723 (11)	2570 (15)	22 (3)
C(4)	4901 (14)	2219 (21)	2714 (29)	42 (7)
C(5)	4528 (13)	1789 (20)	3784 (28)	39 (6)
C(6)	4595 (17)	2361 (27)	1633 (37)	60 (9)
C(7)	6145 (11)	3021 (17)	1449 (22)	23 (5)
O(8)	6096 (8)	3692 (13)	990 (17)	36 (4)
C(9)	6219 (9)	3035 (15)	3558 (20)	14 (4)
O(10)	6211 (9)	3669 (15)	4163 (20)	45 (5)
O(11)	7109 (6)	1897 (10)	2254 (13)	15 (3)
C(12)	7620 (10)	2461 (16)	2078 (22)	20 (4)
C(13)	7672 (14)	3105 (21)	2990 (29)	41 (6)
C(14)	7633 (15)	2829 (23)	823 (31)	47 (7)
O(15)	6478 (6)	910 (10)	3578 (13)	14 (3)
C(16)	6555 (12)	855 (18)	4962 (25)	29 (5)
C(17)	6638 (12)	-52 (20)	5291 (26)	34 (6)
C(18)	5973 (15)	1222 (23)	5486 (30)	46 (7)
O(19)	6380 (7)	878 (10)	1345 (14)	20 (3)
C(20)	6255 (12)	722 (19)	73 (26)	32 (6)
C(21)	5766 (20)	1230 (32)	-362 (43)	78 (11)
C(22)	6278 (23)	-142 (36)	-310 (49)	92 (13)
O(23)	7573 (7)	654 (10)	905 (14)	21 (3)
C(24)	7958 (11)	260 (17)	-11 (23)	25 (5)
C(25)	7706 (11)	281 (17)	-1326 (23)	25 (5)
C(26)	8512 (16)	656 (24)	48 (33)	51 (8)
O(27)	7698 (7)	753 (11)	3530 (15)	24 (3)
C(28)	8154 (14)	393 (22)	4303 (29)	42 (6)
C(29)	8745 (13)	605 (20)	3756 (26)	34 (6)
C(30)	8085 (11)	707 (17)	5659 (24)	28 (5)
C(31)	6244 (18)	-2035 (28)	2372 (38)	65 (10)
C(32)	5705 (13)	-709 (19)	2690 (26)	33 (6)
N(33)	6254 (8)	-1104 (13)	2494 (17)	19 (4)
C(34)	6763 (10)	-667 (15)	2416 (21)	20 (4)
C(35)	7356 (11)	-781 (16)	2400 (23)	24 (5)
N(36)	7757 (9)	-1391 (14)	2545 (18)	23 (4)
C(37)	8377 (13)	-1260 (19)	2311 (26)	35 (6)
C(38)	7614 (15)	-2211 (23)	3023 (31)	47 (7)
C(39)	133 (14)	-236 (21)	2119 (29)	40 (6)
C(40)	-81 (17)	-854 (27)	1420 (36)	58 (8)
C(41)	-192 (15)	-1685 (23)	1904 (31)	46 (7)
C(42)	-95 (16)	-1811 (24)	3010 (34)	51 (8)
C(43)	75 (18)	-1162 (28)	3893 (37)	64 (9)
C(44)	246 (13)	-396 (21)	3358 (28)	39 (6)

Table XIV. Fractional Coordinates and Isotropic Thermal Parameters for $[W(O\text{-}i\text{-}Pr)_3(py)(\mu\text{-}OCCNEt_2)]_2$

atom	10^4x	10^4y	10^4z	$10B_{iso}$, Å^2
W(1)	4051.0 (5)	446.3 (2)	3253.7 (4)	14
O(2)	6433 (8)	349 (4)	5868 (6)	18
C(3)	5639 (12)	598 (5)	4853 (9)	14
C(4)	5542 (12)	1186 (6)	4270 (9)	17
N(5)	6205 (11)	1797 (5)	4561 (8)	20
C(6)	7353 (14)	1890 (6)	5738 (10)	24
C(7)	8850 (14)	1588 (7)	5950 (11)	30
C(8)	5801 (15)	2389 (6)	3788 (10)	24
C(9)	7054 (17)	2623 (7)	3535 (12)	33
N(10)	2167 (10)	-235 (4)	1853 (7)	15
C(11)	2298 (13)	-449 (6)	946 (10)	25
C(12)	1148 (15)	-819 (7)	37 (11)	30
C(13)	-113 (15)	-952 (6)	128 (12)	30
C(14)	-234 (14)	-755 (7)	1111 (11)	28
C(15)	931 (13)	-384 (6)	1946 (10)	23
O(16)	5231 (9)	-223 (4)	2916 (7)	22
C(17)	6664 (12)	-525 (6)	3591 (10)	22
C(18)	7833 (15)	-71 (8)	3542 (14)	38
C(19)	6684 (15)	-1234 (7)	3153 (13)	37
O(20)	2277 (9)	880 (4)	3171 (7)	22
C(21)	1910 (14)	1488 (7)	3619 (11)	27
C(22)	1679 (16)	2078 (7)	2824 (13)	38
C(23)	537 (17)	1342 (9)	3780 (14)	46
O(24)	3845 (8)	923 (4)	1872 (7)	19
C(25)	4767 (13)	1263 (6)	1489 (9)	19
C(26)	3982 (14)	1914 (7)	808 (11)	27
C(27)	5204 (15)	794 (7)	757 (12)	32

drogen atom positions were visible in a difference Fourier phased on the non-hydrogen parameters. The positions of all hydrogens were calculated and placed in fixed idealized positions (d(C–H) = 0.95 Å) for the final cycles. The hydrogen atoms were assigned a thermal parameter of 1 + B_{iso} of the carbon atom to which they were bound.

Acknowledgment. We thank the Department of Energy, Office of Basic Sciences, Chemistry Division for support.

Registry No. I, 101077-90-1; II, 104979-60-4; IIIa, 120411-02-1; IIIb, 120411-01-0; IV, 120416-94-6; $(t\text{-BuO})_3W{\equiv}CNMe_2$, 103946-66-3; $[(t\text{-BuO})_3W{\equiv}CMe]_2$, 86669-24-1; $[(t\text{-BuO})_3WCNMe_2]_2$, 86767-54-6; $(i\text{-PrO})_3WcNMe_2(py)_2$, 104269-39-8; $(O\text{-}i\text{-Pr})_3W{\equiv}CNEt_2(py)_2$, 120411-00-9.

Supplementary Material Available: Listings of anisotropic coordinates and complete listings of bond distances and angles (14 pages); listings of F_o and F_c values (35 pages). Ordering information is given on any current masthead page.

Redox-Induced Arene Hapticity Change in a Mixed-Sandwich Rhodium(III/II/I) System: An Illustrative Mechanistic Application of Electron-Exchange Kinetics

Roger M. Nielson and Michael J. Weaver*

Department of Chemistry, Purdue University, West Lafayette, Indiana 47907

Received September 20, 1988

Rate constants for homogeneous self-exchange, k_{ex}^h, and electrochemical exchange, k_{ex}^e, have been measured for the first and second reduction steps of $(\eta^5\text{-}C_5Me_5)(\eta^6\text{-}C_6Me_6)M^{2+}$, where M = Rh and Co, in order to assess the manner in which the $\eta^6 \rightleftarrows \eta^4$ arene hapticity change observed upon formation of the Rh(I) two-electron reduction product is coupled with electron transfer. The analogous Co(III/II/I) mixed-sandwich system was chosen for comparison because, unlike Rh(III/II/I), the arene retains the η^6 configuration upon reduction. The k_{ex}^h values were evaluated in acetone, acetonitrile, and benzonitrile by utilizing the proton NMR line-broadening technique, and the k_{ex}^e values were obtained in these solvents and also nitrobenzene and propylene carbonate by using phase-selective ac voltammetry at an annealed gold electrode. The corresponding variations in k_{ex}^h and k_{ex}^e with the redox couple are shown to be uniformly consistent with the expectations of Marcus theory, indicating that the electrochemical as well as homogeneous-phase exchange kinetics refer to outer-sphere pathways, as desired. Both the Rh(III/II) and Rh(II/I) couples exhibit smaller rate constants in a given solvent than the corresponding cobalt systems; while these differences are mild for the former couple, the rate constants for Rh(II/I) are substantially smaller (ca. 10^4-fold for k_{ex}^h) than for the other reactions. These rate differences indicate that the redox-induced hapticity change is coupled primarily to the second reduction step. Distinction is made between "square-scheme" mechanisms where the ligand conformational change is coupled to, but is microscopically separate from, the electron-transfer step and "concerted" reaction pathways where the arene distortion forms part of the elementary electron-transfer barrier. Evidence that the mechanism for Rh(II/I) is partly concerted in nature is obtained from an analysis of the solvent dependence of k_{ex}^e, based on the anticipated influence of the ligand distortion in the electron-transfer barrier-crossing frequency. The stabilization afforded to Rh(I) by the $\eta^6 \rightarrow \eta^4$ conformational change is ascertained to be at least 6 kcal mol^{-1}.

The factors giving rise to, and the attendant energetics of, changes in hapticity of metal arenes is a topic of substantial interest, especially given the likely relevance of such ring slippage to ligand substitution chemistry and the catalysis of arene hydrogenation.[1,2] The observed arene ring slippage from hexahapto (η^6) to tetrahapto (η^4) bonding can generally be understood in terms of the consequent attainment of the 18-electron configuration by the metal.[1b] Not surprisingly, therefore, there are several documented examples of such η^6 to η^4 hapticity changes triggered by two-electron reduction of appropriate metal arenes.[3-5] Besides the virtues of redox-induced reactions for preparative purposes, the elucidation of the mechanisms and energetics of the ligand structural transformations is of obvious fundamental importance.

One system of particular interest from this standpoint is provided by the reduction of (η^5-pentamethylcyclopentadienyl)(η^6-hexamethylbenzene)rhodium(III) $[(\eta^5\text{-}C_5Me_5)(\eta^6\text{-}C_6Me_6)Rh^{2+}$, Me = methyl].[4,5] Two-electron reduction of this complex yields the η^4 Rh(I) complex $(\eta^5\text{-}C_5Me_5)(\eta^4\text{-}C_6Me_6)Rh$, similar to several related ruthenium and iridium complexes (see Figure 1).[3-5] However, an unusual feature of the rhodium(III) complex is that it undergoes reduction via two electrochemically resolvable one-electron steps.[4,5] This situation prompts the intriguing question of how the hapticity change, itself involving effectively a two-electron subtraction from the metal center, is coupled to these *single-electron* redox steps.

Several possibilities can be considered. Besides the general distinction between arene conformation changes that are triggered by the first or second (or both) reduction steps, the nature of this coupling is expected to be different depending on whether or not such arene structural alterations occur separately from the elementary electron-transfer barrier itself. That is, it is possible that the ligand conformational change can constitute a microscopically

(1) (a) Muetterties, E. L.; Bleeke, J. R. *Acc. Chem. Res.* **1979**, *12*, 324. (b) Muetterties, E. L.; Bleeke, J. R.; Wucherer, E. J.; Albright, T. A. *Chem. Rev.* **1982**, *82*, 499.

(2) For example: (a) Landis, C. R.; Halpern, J. *Organometallics* **1983**, *2*, 840. (b) Traylor, T. G.; Stewart, K. J.; Goldberg, M. J. *J. Am. Chem. Soc.* **1984**, *106*, 4445.

(3) (a) Kang, J. W.; Childs, R. F.; Maitlis, P. M. *J. Am. Chem. Soc.*, **1970**, *92*, 720. (b) Barbati, A.; Colderazzo, F.; Poli, R.; Zanozzi, P. F. *J. Chem. Soc., Dalton Trans.* **1986**, 2569. (c) Finke, R. G.; Voegeli, R. H.; Laganis, E. D.; Boekelhelde, V. *Organometallics* **1983**, *2*, 347.

(4) Bowyer, W. J.; Geiger, W. E. *J. Am. Chem. Soc.* **1985**, *107*, 5657.

(5) Bowyer, W. J.; Merkert, J. W.; Geiger, W. E.; Rheingold, A. L. *Organometallics* **1989**, *8*, 191.

0276-7333/89/2308-1636$01.50/0